

AD-A196 915

AAE 

DTIC FILE COPY

AERONAUTICAL AND ASTRONAUTICAL ENGINEERING DEPARTMENT

Temporal Variations in a CW HF MOPA

L. H. Sentman
Aeronautical and Astronautical
Engineering Department

DTIC
FILE

DTIC
ELECTE
JUN 02 1988
S H D

ENGINEERING EXPERIMENT STATION, COLLEGE OF ENGINEERING, UNIVERSITY OF ILLINOIS, URBANA

DISTRIBUTION STATEMENT A
Approved for public release;
Distribution Unlimited

88 5 31 2 32

4

Aeronautical and Astronautical Engineering Department
University of Illinois at Urbana-Champaign
Urbana, IL

Technical Report AAE 88-5
UILU ENG 88-0505

Temporal Variations in a CW HF MOPA

L. H. Sentman
Aeronautical and Astronautical
Engineering Department

DTIC
SELECTED
JUN 02 1988
S H D

Prepared for
Defense Advanced Research Projects Agency
1400 Wilson Boulevard
Arlington, VA 22209

Final Report Contract N00014-85-K-0326
1 April 1985 - 30 September 1987

DISTRIBUTION STATEMENT A
Approved for public release
Distribution Unlimited

ADA196915

REPORT DOCUMENTATION PAGE		READ INSTRUCTIONS BEFORE COMPLETING FORM
1. REPORT NUMBER AAE 88-5 UILU ENG 88-0505	2. GOVT ACCESSION NO.	3. RECIPIENT'S CATALOG NUMBER
4. TITLE (and Subtitle) Temporal Variations in a cw HF MOPA		5. TYPE OF REPORT & PERIOD COVERED Final Report 4/1/85 - 9/30/87
7. AUTHOR(s) L. H. Sentman		6. PERFORMING ORG. REPORT NUMBER
9. PERFORMING ORGANIZATION NAME AND ADDRESS Aeronautical & Astronautical Engineering Dept. University of Illinois at Urbana-Champaign Urbana, IL 61801		8. CONTRACT OR GRANT NUMBER(s) N00014-85-K-0326
11. CONTROLLING OFFICE NAME AND ADDRESS Defense Advanced Research Projects Agency 1400 Wilson Boulevard Arlington, VA 22209		10. PROGRAM ELEMENT, PROJECT, TASK AREA & WORK UNIT NUMBERS
14. MONITORING AGENCY NAME & ADDRESS (if different from Controlling Office) Office of Naval Research Resident Representative Room 286, 536 South Clark Street Chicago, IL 60605		12. REPORT DATE May, 1988
		13. NUMBER OF PAGES
15. DISTRIBUTION STATEMENT (of this Report) UNLIMITED		15. SECURITY CLASS. (of this report) UNCLASSIFIED
17. DISTRIBUTION STATEMENT (of the abstract entered in Block 20, if different from Report)		15a. DECLASSIFICATION/DOWNGRADING SCHEDULE
16. SUPPLEMENTARY NOTES		
19. KEY WORDS (Continue on reverse side if necessary and identify by block number) Master oscillator/power amplifier Time-dependent oscillations in cw power Zero power gain Amplifier performance		
20. ABSTRACT (Continue on reverse side if necessary and identify by block number) The experimental and theoretical studies directed toward characterizing the output of a cw HF oscillator/amplifier (MOPA) configuration are summarized. Scale effects when the size of a cw HF chemical laser was reduced by a factor of two were studied experimentally and theoretically. When the saturated gains of the single channel CL I laser and the two channel CL II laser were the same, the CL I power was 70-80% of the CL II power. This suggests that for only a 25% performance penalty, the size, weight and gas requirements of a laser can		

be reduced by a factor of two. The power spectral distributions of the CL I and CL II lasers when the saturated gains were the same were nearly identical. When the two lasers had the same cavity losses, the CL I power was an average of 45% of the CL II power. The Blaze II and MNORO3SR laser computer simulations gave good agreement with data as a function of mass flow rate, cavity losses, pressure and size of the laser. Time-dependent oscillations on lines whose saturated gain did not fill the unstable resonator had a period of 47 ns. These oscillations did not occur for Fresnel numbers less than 3.2 and their amplitudes increased as the fraction of the resonator filled by the saturated gain of the oscillating line decreased. A 7 ns oscillation, which was superimposed on top of the 47 ns oscillation, was probably a mode beat of the laser.

A mechanism for the observed time-dependent oscillations that occur on lines whose saturated gain does not fill the unstable resonator was proposed. According to the proposed mechanism, the time-dependent oscillations are the result of a competition between chemical pumping and radiative deactivation of upper laser levels of HF. The oscillations occur only if the media is not strongly coupled to the optical fields diffractively or geometrically. Computer calculations supported the proposed mechanism and new unstable resonator experiments were suggested.

Inadequacies in the treatment of the fluid dynamic mixing that were not apparent in Fabry-Perot or stable resonator models were revealed with a wave optics unstable resonator model. The unstable resonator data as a function of resonator size and size of the laser were shown to provide a severe test of a coupled, wave optics, chemical kinetic, fluid dynamic model of a chemical laser.

The multiline and single-line amplifier performance of a two channel Helios CL II laser was studied. Flow channel aperturing of the input beam was found to cause a significant reduction in the measured amplification ratio. The absorption of the multiline input beam by SF₆ was found to be negligible (< 0.5% / cm). Maximum multiline and single line amplification was obtained when the input beam was passed through the amplifier at the X₀ corresponding to maximum zero power gain. Single-line amplification ratios were considerably lower than multiline amplification ratios obtained for the same input power. The P₂(6) amplification ratios were lower than the P₁(6) amplification ratios, even though the P₂(6) zero power gain was considerably higher than the P₁(6) zero power gain. The data suggested that about 1/3 of the oscillator output needs to be input to obtain amplifier output equal to the device's oscillator performance.

Low pressure (5-7 torr) P₂(J) peak zero power gains were about 1.55 times larger than the P₁(J) peak zero power gains. The zero power gain zones of the P₁(J) lines were about 1.3 times longer than those of the P₂(J) lines. The zero power gains of all the P₁(J) lines peaked 1.5 - 2.0 mm downstream of the H₂ injectors while the zero power gains of the P₂(J) lines peaked 1.0 mm downstream of the H₂ injectors. The lines with the highest zero power gains were P₁(5) and P₁(6) for the 1 → 0 vibrational band and P₂(5) and P₂(6) for the 2 → 1 vibrational band. High pressure (10-12 torr) did not affect the peak P₁(6) zero power gain but caused a 22.5% decrease in the peak P₂(5) and P₂(6) gains. The gain zones were shortened by 46.7%. Zero power gain measurements obtained with vertically polarized, horizontally polarized and unpolarized beams showed that polarization does not affect zero power gain.

TABLE OF CONTENTS

I. INTRODUCTION.....1

II. SCALE EFFECTS IN CW CHEMICAL LASERS.....2

III. UNSTABLE RESONATOR PERFORMANCE.....5

 3.1 COMPUTER SIMULATION OF UNSTABLE RESONATOR PERFORMANCE.....5

 3.2 PROPOSED MECHANISM FOR THE TIME-DEPENDENT
 OSCILLATIONS IN AN UNSTABLE RESONATOR.....11

IV. AMPLIFIER PERFORMANCE.....15

V. CONCLUDING REMARKS.....26

REFERENCES.....33

DTIC
COPY
INSPECTED
4

Accession For	
NTIS GRA&I	<input checked="" type="checkbox"/>
DTIC TAB	<input type="checkbox"/>
Unannounced	<input type="checkbox"/>
Justification	
By _____	
Distribution/	
Availability Codes	
Dist	Avail and/or Special
A-1	

I. INTRODUCTION

This research is an integrated experimental and theoretical investigation of the multi-line issues associated with assessing the impact of temporal variations in a CW HF device on the capability of achieving a phased output beam from multiple laser cavities. The objectives of this research are to fully characterize the output of an oscillator-amplifier (MOPA) configuration as a function of the oscillator input beam, time-dependent oscillations, mode beats, and determine if the coupling between the oscillator and amplifier perturbs the oscillator output; these studies are to be carried out for first one and then two amplifiers driven by the same oscillator. To accomplish these objectives, the flow fields in the oscillator and amplifiers must be identical; to ensure that this is so, the devices must first be fully characterized as oscillators (power, power spectral distributions, beam diameters, time-dependent oscillations as a function of cavity losses, pressure and flow rates) including simulation of their performance with computer models. This background information is essential to the interpretation and guidance of the MOPA experiments.

The major results of the research program are summarized. The details are contained in References 1-5. In the next section, the results of the comparative study of the performance of the single and two channel lasers is presented. In Section III, the results of the modeling of unstable resonator performance is described and the mechanism responsible for the time-dependent oscillations which may occur on lines whose saturated gain does not fill the unstable resonator is summarized. The multi and single line amplifier performance as a function of input power and polarization is described in Section IV. In the last section, several concluding remarks are presented.

II. SCALE EFFECTS IN CW CHEMICAL LASERS

The two channel Helios CL II cw HF chemical laser, which was used as the amplifier, was fully characterized in a previous study of the time-dependent oscillations which occur on lines whose saturated gain does not fill the unstable resonator⁶⁻¹³. The flow channel in the single channel Helios CL I cw HF laser, which was used as the oscillator, is identical to one of the flow channels in the two channel laser which was used as the amplifier. Thus, when the CL I is run at one half the mass flow rates¹ of the CL II, the flow fields in the oscillator and amplifier are identical. The objective was to fully characterize the Helios CL I single channel laser as an oscillator. To facilitate comparison with the CL II data, power, power spectral distributions, beam diameters, and time-dependent oscillations as a function of cavity losses, pressure and flow rates were measured² for the same range of parameters for which the CL II data were taken.

Several scale effects were observed² when comparing CL I stable resonator data with CL II stable resonator data, Table 1. When the resonators have the same cavity losses, the CL I power was an average of 45% of the CL II power. The slopes of the power versus reflectivity curves are steeper for the CL II than for the CL I, except for the high pressure, highest SF₆ flow rates. The spectral peaks of the CL I laser are shifted one J lower than the spectral peaks of the CL II laser. The CL I spectra show the appearance of lower J lines and the loss of higher J lines when compared to CL II spectra having the same cavity loss. Fewer lines are observed in the power spectral distributions of the CL I laser. The beam diameters of the CL I laser are smaller than those of the CL II laser. These scale effects are all pressure independent and are a consequence of the CL I laser having twice the saturated gain of the CL II laser.

Same Cavity Loss

	RUN NO.					
	32	33	34	35	36	37
Low Pressure						
CL I, $r_{\text{eff}} = 0.46$	25.4	16.7	11.7	28.0	18.2	12.6
CL II, $r_{\text{eff}} = 0.46$	49.1	42.2	30.6	51.7	44.2	32.8
% (CL I / CL II)	51.7	39.6	38.2	54.2	41.2	38.4
High Pressure						
CL I, $r_{\text{eff}} = 0.46$	17.8	15.0	9.0	20.0	16.7	10.3
CL II, $r_{\text{eff}} = 0.46$	37.0	32.8	23.3	40.0	34.7	25.9
% (CL I / CL II)	48.1	45.7	38.6	50.0	48.1	39.8

Overall Average % (CL I / CL II) = 44.5

Same Saturated Gain

Low Pressure						
CL I, $r_{\text{eff}} = 0.63$	33.2	21.6	15.3	35.7	23.0	15.5
CL II, $r_{\text{eff}} = 0.39$	43.7	37.5	28.2	46.2	40.2	29.6
% (CL I / CL II)	76.0	57.6	54.3	77.3	57.2	52.4
High Pressure						
CL I, $r_{\text{eff}} = 0.63$	25.0	19.2	13.1	30.3	22.0	14.0
CL II, $r_{\text{eff}} = 0.39$	35.5	30.5	20.6	38.0	32.5	22.1
% (CL I / CL II)	70.4	63.0	63.6	79.7	67.7	63.3

Overall Average % (CL I / CL II) = 65.2

Table 1. Comparison of the measured Helios CL I and CL II stable resonator total powers when the cavity losses are the same and when the saturated gains are the same for low and high pressure.

Different scale effects are observed² when the CL I and CL II resonators have the same saturated gain, Table 1. The CL I power varied from 52-80% of the CL II power; for the high SF₆ flow rates, the CL I power was 70-80% of the CL II power. These data indicate that if the saturated gain is kept constant as the size of the laser is reduced, it may be possible to reduce the size, weight and gas flow rates by a factor of two with only a 25% performance penalty. The power spectral distributions of the two resonators having the same saturated gain are similar, including the minimum^{6,7} at P₂(11) for high pressure. This minimum is thought to be a consequence of a near resonant energy transfer from v = 3, J = 3,4 to v = 2, J = 14 with a subsequent rotational cascade to v = 2, J = 11. The beam diameters of the CL I laser are smaller than those of the CL II laser. The difference between the beam diameters of the CL I and II lasers when the saturated gains are the same is less than when the two resonators have the same cavity loss. For the same saturated gain case, the difference between CL I and CL II beam diameters is a result of the different mirror separations which occurred when EMM (external mirror mounts) were used on the CL II and VMM (vacuum mirror mounts) on the CL I.

To verify the ability of the BLAZE II¹⁴ and MNORO3SR¹² computer simulations of the Helios laser to predict performance as the size of the laser changes, CL I simulations were made by having the input mass flow rates and gain length of the CL II laser. The results of these calculations² gave good agreement with the measured CL I power, power split and beam diameters. MNORO3SR computations produced power spectral distributions which are in reasonable agreement with the CL I data. These calculations show that the BLAZE II and MNORO3SR simulations of the Helios laser are valid as a function of mass flow rates, cavity losses, pressure and size of the laser.

To complete the characterization of the CL I laser, the CL I was run with an unstable resonator. These experiments used the same 50% geometric outcoupled, confocal, unstable resonator that was used in the CL II experiments⁸. A variable slit scraper mirror was used to outcouple the power and allowed the Fresnel number to vary from 0.0 to 35.7. The time-dependent oscillations in the output beam of the CL I unstable resonator, Fig. 1, all had a period of about 47 ns and increased in amplitude as the fraction of the resonator filled by the saturated gain of a lasing line decreased. A 7 ns oscillation, which was superimposed on top of the 47 ns oscillation, is thought to be a mode beat of the laser. The oscillations on lines whose saturated gain does not fill the resonator did not occur for Fresnel numbers less than 3.2. Comparison of CL I and CL II unstable resonator data showed that fewer lines were observed for the CL I which is a consequence of the saturated gain of the CL I being twice as large as that of the CL II.

III. UNSTABLE RESONATOR PERFORMANCE

3.1 COMPUTER SIMULATION OF UNSTABLE RESONATOR PERFORMANCE

Computer simulation of chemical laser performance must adequately model three coupled elements of chemical laser physics. These elements are the fluid dynamics of the flow field, including the fluid dynamic mixing of the fuel and oxidizer streams, the chemical kinetics occurring in the fluid media, and the optical resonator. The computer simulation of the Helios CL II and CL I, arc driven, subsonic, continuous wave HF chemical lasers is accomplished with the computer codes BLAZE II^{14,15}, MNORO3¹¹, MNORO3SR^{12,13} and MNORO3UR¹². The MNORO3, MNORO3SR and MNORO3UR codes are rotational nonequilibrium models with Fabry-Perot, stable resonator geometric optics, and unstable resonator wave optics models, respectively. The BLAZE II code is a

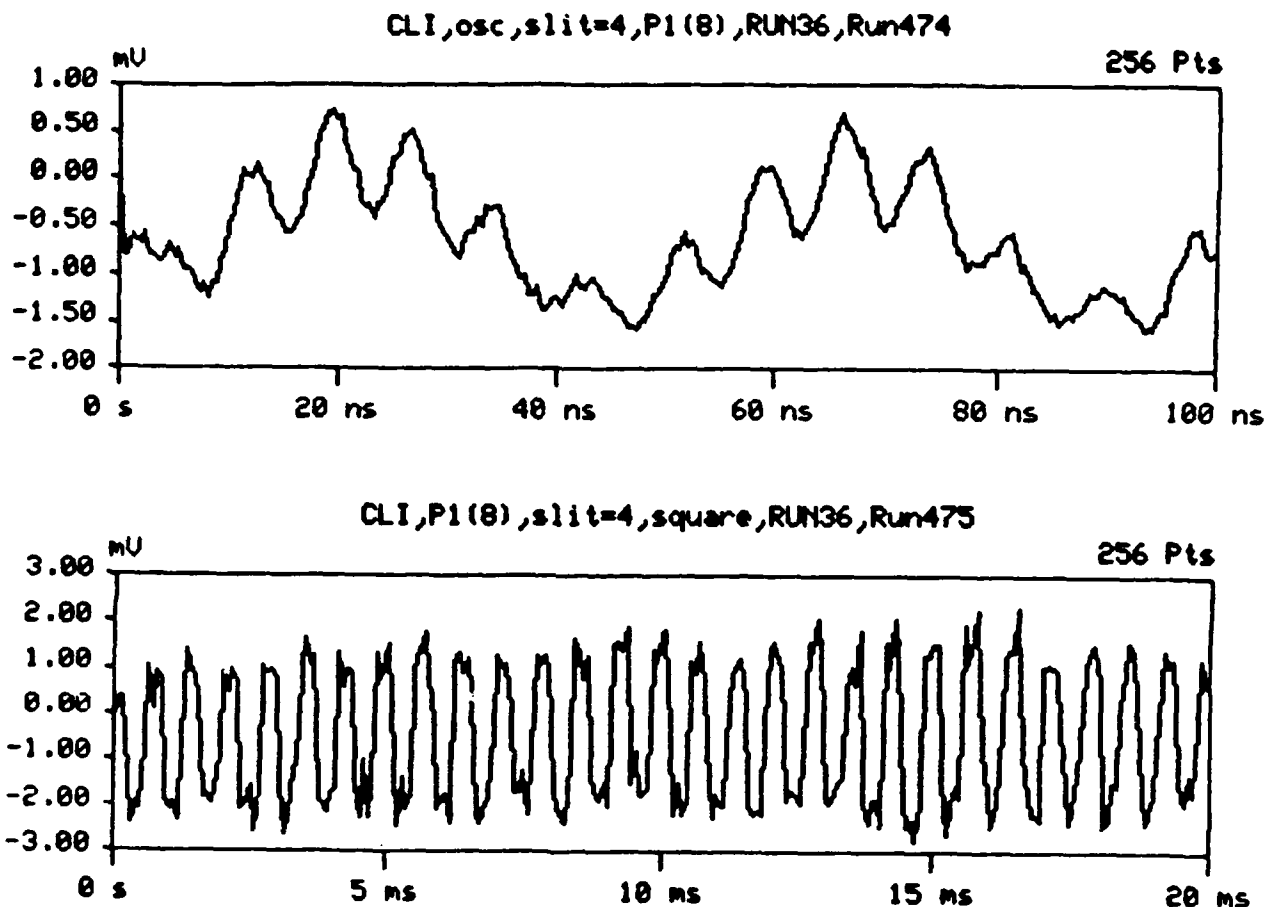


Figure 1. Typical oscilloscope traces of the time-dependent oscillation on a line whose saturated gain does not fill the unstable resonator. These data are for the $P_1(8)$ line for a scraper mirror slit width of 4 mm for the RUN 36 flow rates at 6.5 torr. The 47 ns oscillation with the superimposed 7 ns oscillation is clearly evident in the upper trace. The lower trace shows the square wave which results from the beam chopper. From the vertical scale of these traces, the percent amplitude modulation induced by the 47 ns oscillation was calculated.

rotational equilibrium, Fabry-Perot model which calculates all fluid dynamic properties from input initial conditions. The BLAZE II code is well suited for the simulation of laser performance in terms of total outcoupled power, power contained in each vibrational band, and the length of the lasing zone. However, since BLAZE II employs rotational equilibrium kinetics, it cannot compute realistic power spectral distributions.

Because BLAZE II is a very inexpensive code to run when simulating chemical laser performance, BLAZE II calculations are always performed first. After suitable agreement between BLAZE II calculations and the data is obtained, the rotational nonequilibrium codes (MNORO3, MNORO3SR, MNORO3UR) are used. In the rotational nonequilibrium codes, profiles for the velocity, temperature, and pressure of the flow, the mass flow remaining in the primary stream, the mass flow remaining in the secondary stream, and the ratio of the thickness of the mixed stream to the geometrical thickness of the flow are input data. These profiles are obtained from a rotational equilibrium model such as BLAZE II.

The flow field in the Helios CL II and CL I laser bodies is a complex three-dimensional flow³, Fig. 2. A sketch of the appearance of the H₂ jets is shown on the left side of Fig. 2. These jets are well defined with the chemical reaction occurring at the interface of the primary (oxidizer) stream and the H₂ jets. The appearance of these jets as seen looking upstream is shown as Section AA in Fig. 2. To treat this complicated three-dimensional mixing, the flow was idealized as a series of alternating primary and secondary (fuel) slit nozzles³ as shown on the right side of Fig. 2. The mixing calculation with BLAZE II was performed utilizing a linear scheduled mixing option^{14,15}.

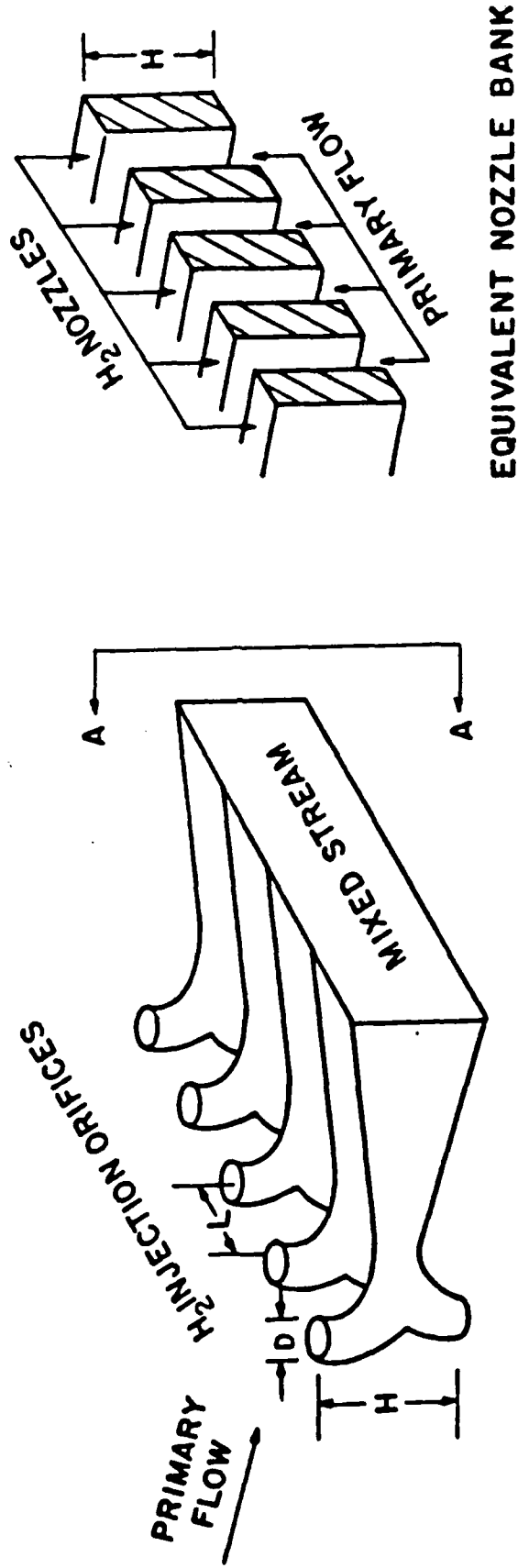


Figure 2. Illustration of the actual mixing geometry and the equivalent nozzle geometry.

The BLAZE II code integrates the governing ordinary differential equations describing the chemical kinetics and fluid dynamics. The integration is performed in the flow direction, starting at the nozzle exit plane. For the Helios CL II and CL I lasers, the nozzle exit plane coincides with the point of H₂ injection¹⁰. The integration requires the specification of all of the dependent variables in the equation set at the nozzle exit plane. For the fluid dynamic equations, the dependent variables that must be specified consist of the static temperature and pressure at the nozzle exit plane, the cross sectional area of the flow channel, the mass flow rates of the primary and secondary streams, and the chemical composition of the primary and secondary streams. To obtain values for these starting conditions, the static pressure is measured 5 mm downstream of the H₂ injectors and the static pressure at the nozzle exit plane (H₂ injectors) is varied until the pressure 5 mm downstream agrees with the measured value. The cross sectional area of the flow channel and the mass flow rates are measured. The static temperature of the flow at the nozzle exit plane (H₂ injectors) and the mass fractions of F, O₂, SF₆, SF_x (x = 1-5), and SO₂ are unknown. The mass fractions are unknown because the degree to which SF₆ is dissociated in the arc is unknown. In addition to these quantities, the lengths after which the primary and secondary streams are completely mixed must be specified. Thus, to model the Helios CL II and CL I lasers, there are four a priori undetermined quantities that must be specified. The four quantities are the percent SF₆ dissociation in the arc, the static temperature of the flow at the H₂ injectors, the primary mixing length, and the secondary mixing length. A set of these four quantities, called baseline parameters, must be chosen so that the model will accurately predict laser performance. The process of determining the values of these parameters is called baselining.

An objective of this study was to examine unstable resonator modeling in light of Fabry-Perot and stable resonator modeling results which showed that both the Fabry-Perot and stable resonator models needed to be separately baselined to Fabry-Perot and stable resonator data, respectively^{13,16}. The Fabry-Perot model was baselined to Fabry-Perot data because the model did not accurately predict the data when a set of parameters obtained from baselining the Fabry-Perot model to stable resonator data was used. When the baseline parameters determined from baselining Fabry-Perot model to Fabry-Perot data were used in the stable resonator model, the model did not accurately predict stable resonator data. Thus the stable resonator model was baselined to stable resonator data. The separate baselining of the Fabry-Perot and stable resonator models appears to be accounting for some aspect of the resonator modes which is not included in the resonator models^{13,16}. The goal in this study was to determine whether a different set of the four baseline parameters is required to model the unstable resonator data even though the wave optics unstable resonator model includes mode structure.

The results of the unstable resonator baselining process³ indicated that one set of baseline parameters that allow the model to predict unstable resonator data as the size of the resonator and size of the laser varied could not be found. It was, however, possible to obtain different sets of baseline parameters for individual resonator sizes. The best fit parameter set for the 2 mm slit case accurately predicted the total power, but also predicted a 20 nsec small amplitude oscillation that was not seen experimentally. The best fit parameter set for the 4 mm slit case accurately predicted the total power and period of the time-dependent oscillations, but underpredicted the amplitude modulation. The best fit parameter set for the 5 mm slit case was a set of parameters obtained from baselining the Fabry-Perot model to stable

resonator data^{10,17}. This parameter set, used in previous unstable resonator modeling, accurately predicted the period and amplitude of the time-dependent oscillations, but overpredicted the total power. Neither the 2mm slit nor the 4 mm slit baseline parameters predicted scale effects as the size of the laser was reduced by a factor of two.

The instability to obtain one set of baseline parameters for the unstable resonator model demonstrated that the model is inadequate. The limitations imposed by the mixing model did not prevent the Fabry-Perot and stable resonator models from being baselined to the data. This suggested two possible explanations. Since the actual fluid dynamics is independent of the resonator and the unstable resonator model is a more exact treatment of the optics, the wave optics model of the unstable resonator may have brought out inadequacies in the mixing model that were not apparent with geometric optics models. Another possible explanation is that the way in which the optical fields sample the media in an unstable resonator has brought out the inadequacies in the mixing model. Fabry-Perot and stable resonators have no upstream/downstream coupling and full upstream/downstream coupling of the media and optical fields, respectively. The unstable resonator couples upstream of the optical axis and downstream of the optical axis, but not across the optical axis. Both possible explanations demonstrate that unstable resonator data as a function of resonator size and size of the laser provide a severe test of a coupled, wave optics, chemical kinetic, fluid dynamic model of a chemical laser.

3.2 PROPOSED MECHANISM FOR THE TIME-DEPENDENT OSCILLATIONS IN AN UNSTABLE RESONATOR

An objective of this study was to investigate the mechanism responsible for the time-dependent oscillations that occur on lines whose

saturated gain does not fill the unstable resonator. These oscillations have been the subject of several earlier studies^{2,8,10,18}. In these studies, the oscillations were found to occur in both the CL II and CL I lasers at low cavity pressures for resonator Fresnel numbers above a demarcation Fresnel number of 1.5 in the CL II and 3.2 in the CL I. The period of the oscillations was 40 nsec in both the CL II and CL I and was independent of the flow rates. The period of the oscillation was determined by the resonator magnification, and the amplitude modulation was determined by the fraction of the resonator filled by the saturated gain of the lasing line. In addition to the 40 nsec oscillation, a 7 nsec oscillation was superimposed on it. The 7 nsec oscillation corresponds to a mode beat of the laser.

The data showed that the occurrence of the time-dependent oscillations was Fresnel number dependent and that the period of the oscillation was determined by the resonator magnification. Accordingly, a series of unstable resonator MNORO3UR calculations with 4 mm and 5 mm slit resonators were performed to investigate the effect of varying the resonator Fresnel number and the resonator magnification. The resonator magnification was varied through the radii of curvature of the mirrors. The Fresnel number was varied by changing the size of the large mirror. The calculations were performed for the CL II laser for the low pressure Run 34 flow rates. The baseline parameters used were the best fit parameter sets for the 4 mm and 5 mm slit resonators, Sets D and FPSR, respectively. Selected information from the 4 mm and 5 mm slit calculations is presented in Table 2.

The calculations presented in Table 2 showed a correlation between the period of the time-dependent oscillations and the number of passes¹⁹, n_p , for a wave to exit the resonator after leaving the central Fresnel zone. As n_p increased, the period of the time-dependent oscillations increased. The trend

Baseline Parameters	D_L (cm)	D_S (cm)	L (cm)	t_w	M	Geometric Outcoupling	D_{CF} (mm)	N_F	η_p	τ	Amp. mod.
EMM data ^{10,11}	1.0	0.50	100	-----	2.00	50%	---	8.93	---	40	25% P _{total}
FPSR	1.0	0.50	100	1.00	2.00	50%	3.3	9.46	1.6	40	18 to 100%
FPSR	1.0	0.80	100	1.00	1.25	20%	3.3	8.93	4.9	∞	--
EMM data ^{10,11}	0.8	0.40	100	-----	2.00	50%	---	5.71	---	40	20 to 80%
Set D	0.8	0.40	100	0.97	2.00	50%	3.3	5.71	1.3	40	10 to 20%
Set D	0.8	0.52	100	0.97	1.54	35%	3.3	5.71	2.0	60	5%
Set D	0.8	0.64	100	0.97	1.25	20%	3.3	5.71	3.9	∞	--

Table 2. Selected information from MNOR3UR calculations for the CL II laser for the low pressure, Run 34 flow rates for various confocal unstable resonators. D_L is the large mirror diameter. D_S is the small mirror diameter. L is the mirror separation. t_w is the effective Brewster window transmissivity. M is the resonator magnification. D_{CF} is the diameter of the central Fresnel zone. N_F is the resonator Fresnel number. η_p is the number of passes for a wave to exit the resonator after leaving the central Fresnel zone. τ is the calculated period of the time-dependent oscillations. Amp. mod. is the calculated single line amplitude modulation of the time-dependent oscillations.

was evident in both the 4 mm and 5 mm slit calculations. This correlation between the number of passes for a wave to exit the resonator after leaving the central Fresnel zone and the period of the time-dependent oscillations led to the following hypothesis concerning the mechanism responsible for the time-dependent oscillations.

The time-dependent oscillations of the laser power are the result of a competition between chemical pumping and radiative deactivation due to lasing. If, in a given time, radiative deactivation removes more HF molecules from an upper laser level than the chemistry can repopulate, the gain on that line is reduced. The reduced gain results in reduced intensities. Since the stimulated radiative processes are proportional to the intensity, reduced intensities reduce the radiative deactivation rate. The chemical processes, which are independent of the intensity, then catch up and re-establish the population inversion. Once the population inversion is re-established, the entire cycle repeats itself.

The data and the MNORO3UR calculations in Table 2 indicated that strong coupling, either diffractive or geometric, prevented the oscillations by locking the media and the optical fields together. Strong geometric coupling occurs when the photons require several passes to exit the resonator. Strong diffractive coupling occurs when the Fresnel number is small. Thus, for the oscillations to occur, the rate of chemical pumping must be less than the rate of radiative deactivation, and the media must not be strongly coupled to the optical fields either diffractively or geometrically.

Computer calculations with the unstable resonator model supported the proposed mechanism³. The calculations showed that the oscillations were damped by increasing the rate of the chemical pumping reactions, and the

period was increased by increasing the degree of coupling between the media and the optical fields.

IV. AMPLIFIER PERFORMANCE

The objectives were to perform a preliminary experimental investigation of the performance of a cw HF amplifier, to experimentally determine the zero power gains of several lines in the amplifier and to examine the effect of polarization on zero power gain. A single channel Helios CL I cw HF chemical laser was used as the oscillator and a two channel Helios CL II cw HF chemical laser was used as the amplifier. The flow channel in the single channel Helios CL I laser is identical to one of the flow channels in the two channel Helios CL II laser. Thus, when the CL I is run at one half the mass flow rates of the CL II, the flow fields in the oscillator and amplifier are identical.

Comparison of the 0% and 50% aperturing data for the same oscillator/amplifier flow rate combinations showed that aperturing of the input beam by the amplifier flow channel causes a significant reduction (an average of 16.0%) in the amplification ratio. For this reason, all data were taken with no flow channel aperturing of the input beam.

The absorption of the multiline input beam by the gases flowing in the primary stream was investigated. It was found that He and O₂ did not absorb, but SF₆ did. The absorption due to SF₆ was quite small (< 0.5% / cm), and thus its effect on amplifier performance was neglected.

Multiline amplification experiments showed that the peak amplification ratios occurred at an X₀ that is both close to the values of X₀ for peak power when a stable resonator is used on the CL II, and close to the values of X₀ at which the peak zero power gains of the P₁(J) and P₂(J) lines were measured⁴,

Fig. 3. Thus, to obtain maximum amplification, the input beam should be passed through the amplifier at the X_0 location corresponding to peak amplifier gain. Higher amplification ratios were obtained when both the oscillator and the amplifier were run at the Run 34 flow rates than when both were run at the Run 36 flow rates. This was a consequence of the higher input intensity that was used in the case of the Run 36 flow rates.

Single-line amplification experiments showed that the peak $P_1(6)$ amplification ratio is located at an X_0 of 1.5 mm, which is the same X_0 at which the $P_1(6)$ amplifier zero power gain is maximum. In the case of $P_2(6)$, the maximum amplification ratio occurs 1.0 mm downstream of the H_2 injectors, which is again the location at which the $P_2(6)$ zero power gain reaches its maximum value. Thus, to obtain maximum single-line amplification, the input beam should be passed through the amplifier at the X_0 for maximum zero power gain. The single-line amplification ratios are considerably lower than the multi-line amplification ratios that were measured using the same input power. This is a result of the fact that in the multiline case, the total input power was distributed among the different lasing lines, which means that the input intensity on each line was less than the input intensity in the single-line case. This fact results in higher amplification ratios for each line, because each line's gain in the amplifier was depressed less than in the single-line case for the same total input power. The $P_2(6)$ amplification ratios measured are lower and less sensitive to X_0 than the $P_1(6)$ amplification ratios, even though the $P_2(6)$ zero power gain is considerably higher and more sensitive to X_0 than the $P_1(6)$ zero power gain.

The multiline MOPA performance was investigated as a function of input power, Fig. 4. It was found that about 1/3 of the oscillator output needs to

HELIOS CL II Single Pass Amplifier

Low Pressure Multi Line

Flow Rates: OSC Run 36

AMP Run 36

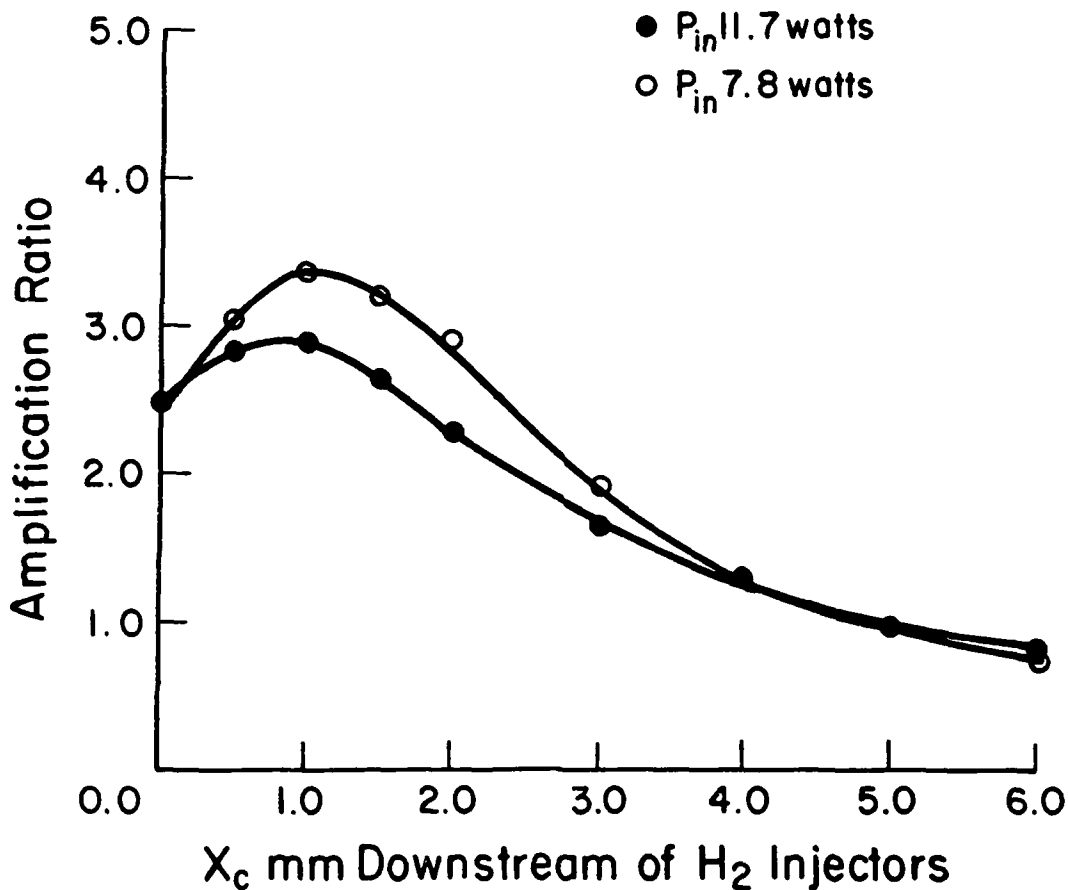


Figure 3. Amplification ratio as a function of the location of the axis of the input beam with respect to the H_2 injectors for zero flow channel aperturing of the input beam.

Amplifier performance at the X_c for peak amplification

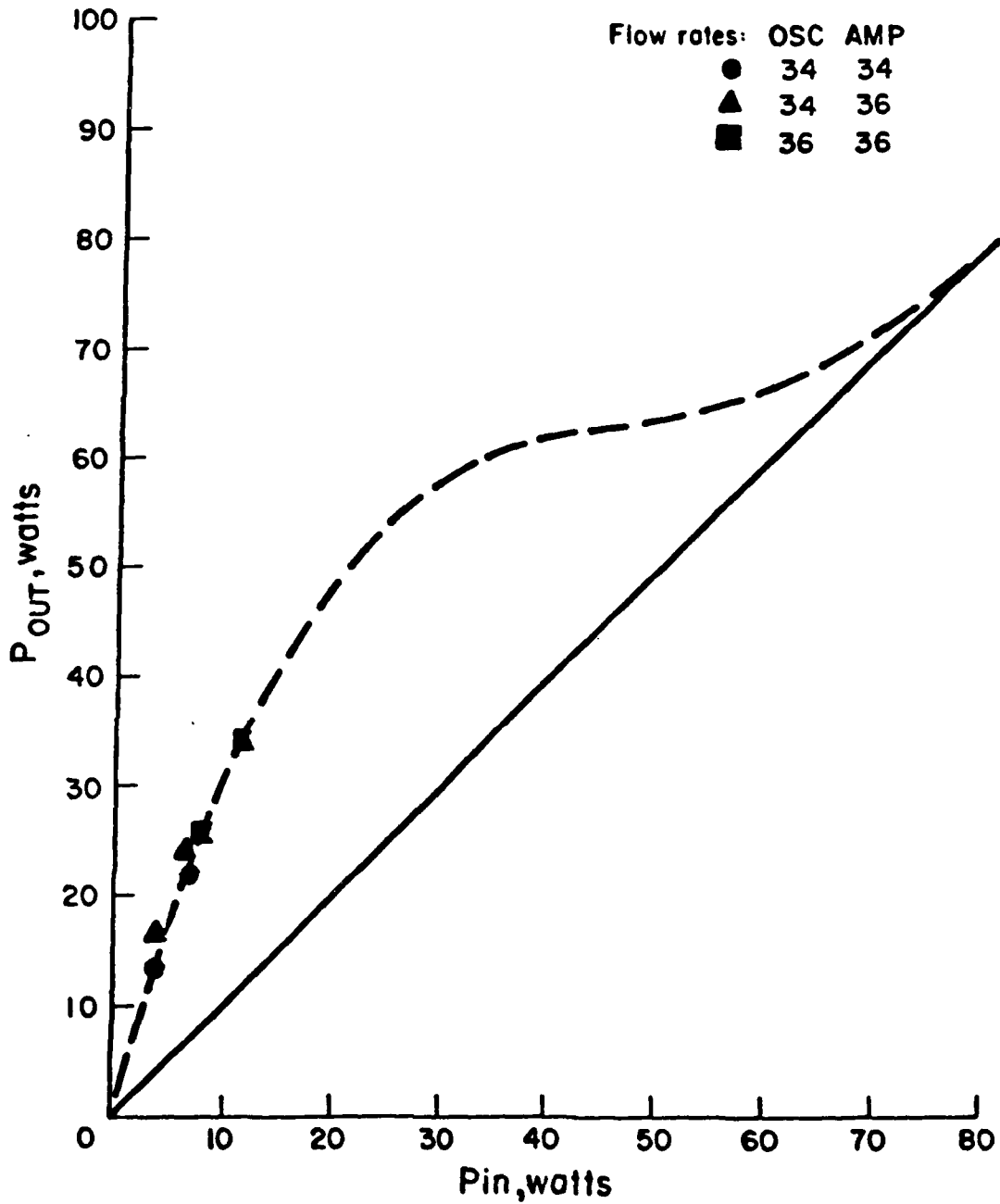


Figure 4. P_{OUT} versus P_{IN} at the X_c for peak amplification for several oscillator/amplifier flow rate combinations.

be input to obtain amplifier output equal to the CL II's oscillator performance.

Low pressure zero power gain data showed that the $P_2(J)$ peak zero power gains are about 1.55 times larger than the $P_1(J)$ peak zero power gains, Figs. 5-8. The length of the gain zone of the $P_1(J)$ lines is about 1.3 times larger than that of the $P_2(J)$ lines. The zero power gains of all the $P_1(J)$ lines reach their peak 1.5 - 2.0 mm downstream of the H_2 injectors while the zero power gains of the $P_2(J)$ lines reach their peak 1.0 mm downstream of the H_2 injectors. The locations of both the $P_1(J)$ and the $P_2(J)$ peak zero power gains are close to the location of the optical axis for peak power when the CL II was run as an oscillator with a stable resonator²⁰. The lines with the highest zero power gains are $P_1(5)$ and $P_1(6)$ for the $1 \rightarrow 0$ vibrational band and $P_2(5)$ and $P_2(6)$ for the $2 \rightarrow 1$ vibrational band.

The variation of zero power gain with height in the flow channel was investigated and it was found that the zero power gain values obtained 0.75 mm above and 0.75 mm below the center of the flow channel are almost identical and higher than the values of the zero power gain measured on the flow channel centerline. This is due to the way the primary and the secondary streams mix after injecting H_2 from the upper and lower flow channel walls.

The effect of high pressure on zero power gain was investigated for lines $P_1(6)$, $P_2(5)$ and $P_2(6)$. It was found that high pressure results in zero power gain zones that are considerably shorter than those measured in the case of low pressure. The peak zero power gain of $P_1(5)$ and $P_2(6)$ were decreased by about 22.5%. This is a result of the fact that the increased deactivation of HF(2) repopulates HF(1) thereby keeping the population difference between HF(1) and HF(0) about the same whereas the population difference between HF(2)

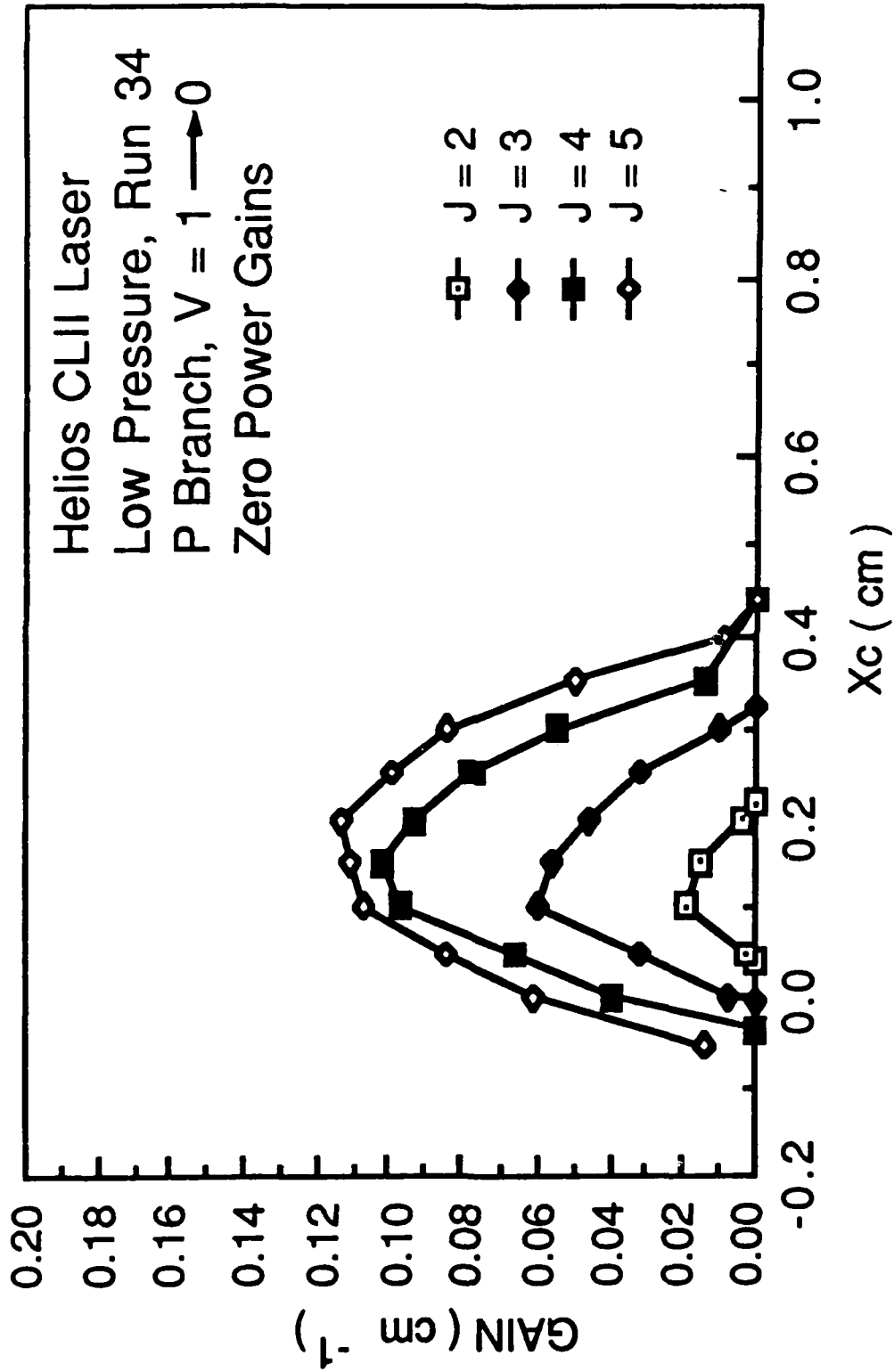


Figure 5. Variation of the zero power gain as a function of distance downstream of the H₂ injectors at y = 0.75 mm for several P₁(J) lines. Error bars smaller than the symbols are not shown.

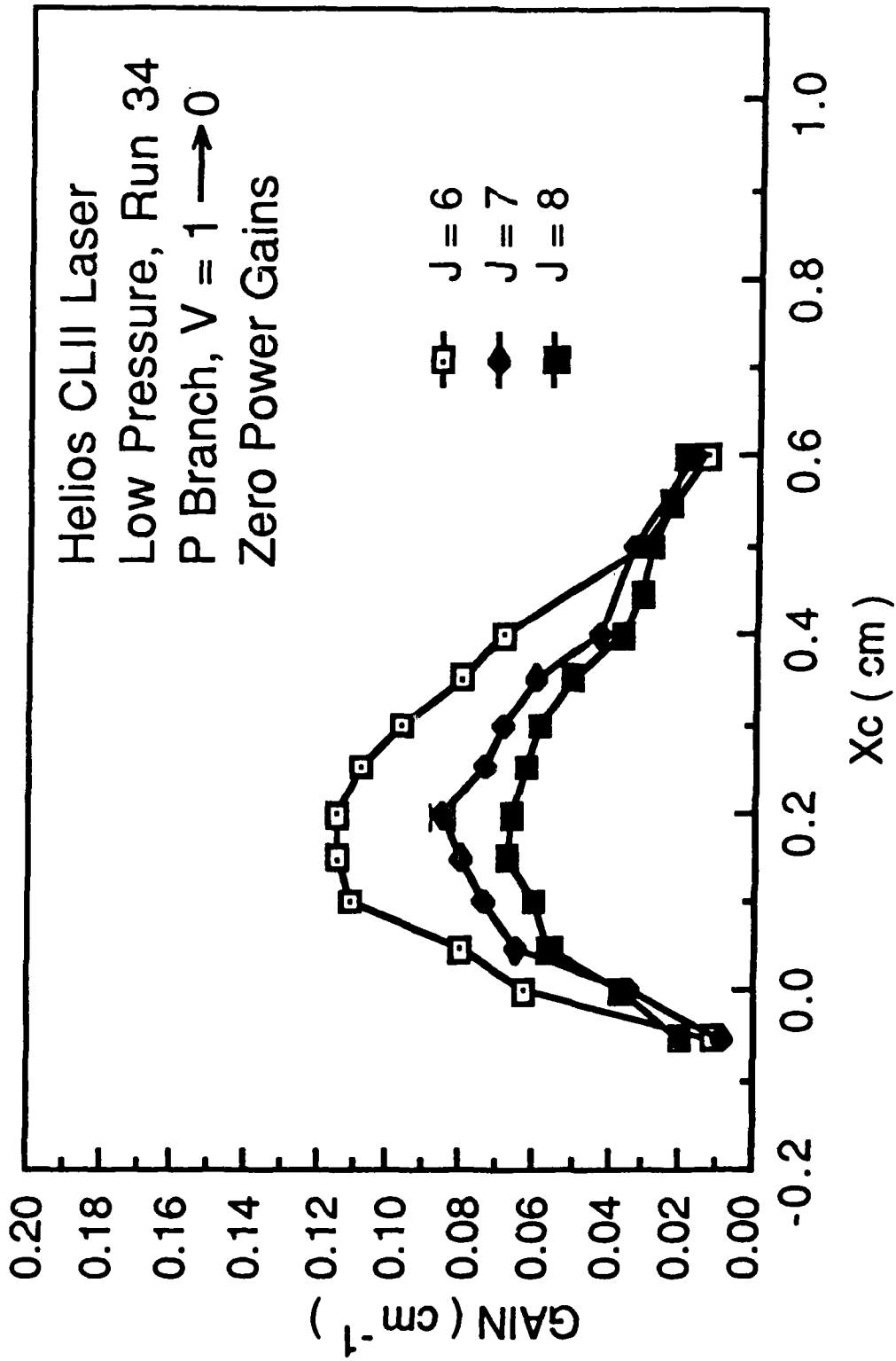


Figure 6. Variation of the zero power gain as a function of distance downstream of the H_2 injectors at $y = 0.75$ mm for several $P_1(J)$ lines. Error bars smaller than the symbols are not shown.

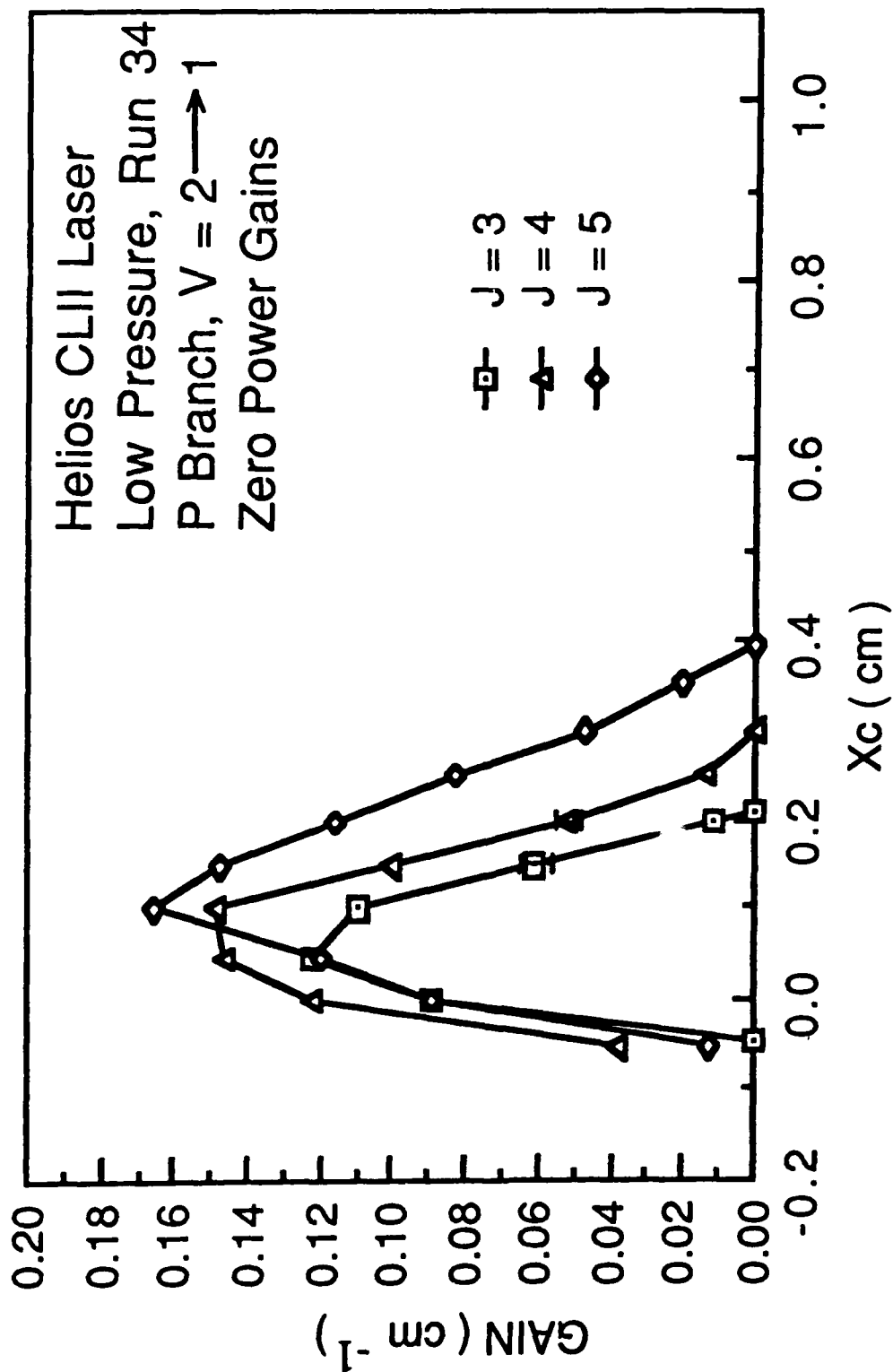


Figure 7. Variation of the zero power gain as a function of distance downstream of the H_2 injectors at $y = 0.75$ mm for several $P_2(J)$ lines. Error bars smaller than the symbols are not shown.

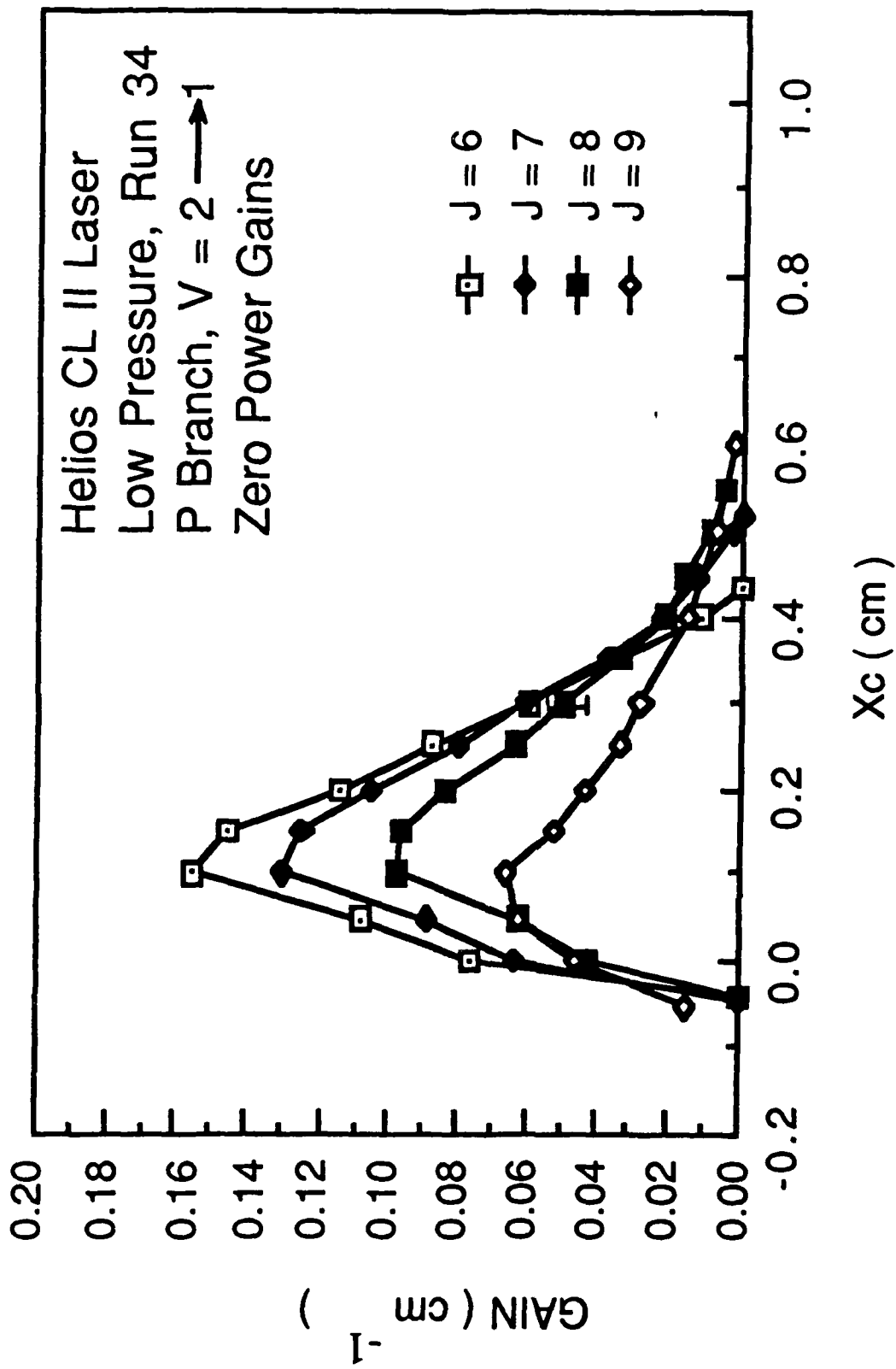


Figure 8. Variation of the zero power gain as a function of distance downstream of the H₂ injectors at y = 0.75 mm for several P₂(J) lines. Error bars smaller than the symbols are not shown.

and HF(1) decreased. High pressure caused the location of the peak zero power gain to occur 0.5 mm closer to the H₂ injectors for all three lines.

The effect of polarization on zero power gain was investigated by using an unpolarized and a horizontally polarized input beam and non-Brewster windows on the amplifier. The non-Brewster windows acted as a Fabry-Perot resonator, causing the amplifier to lase on lines P₂(4) and P₂(5). The fact that the lines P₂(4) and P₂(5) lased with the non-Brewster windows on the amplifier supports the zero power gain data because it suggests that P₂(4) and P₂(5) have the highest gains, which is in agreement with the experimental results that show P₂(5) to have the highest zero power gain followed by lines P₂(4) and P₂(6) whose zero power gains were about equal. The amplifier lasing was stopped after tilting the right non-Brewster window by about 0.5 degree. Then gain versus x data was obtained for lines P₁(5), P₁(6), P₂(5) and P₂(6) using an unpolarized beam. Comparison of the gains obtained in this case with the zero power gains of the same lines obtained with a vertically polarized beam showed that the gains obtained with the unpolarized input beam were considerably lower. The gains obtained with the unpolarized beam were lower than the zero power gains obtained with the vertically polarized beam because the right amplifier non-Brewster window reflected (the non-Brewster window reflectivity was calculated to be 3.3%) back into the cavity enough power to cause a significant increase of the average intensity that the media sees. This increased I_{AV} was enough to perturb the media and cause the amplifier gain to decrease from the zero power gain levels measured with a vertically polarized beam to the gains measured with an unpolarized beam. The right amplifier non-Brewster window was then tilted 1.0 degree more, and the gain was measured as a function of x. The gain measured in this case was equal to the zero power gain measured with the Brewster windows on the amplifier. Zero

power gain measurements were then made for lines $P_1(5)$ and $P_2(5)$ using a horizontally polarized input beam. The input powers required for these measurements (in order to reach the zero power gain levels) were considerably lower than the input powers used in zero power gain measurements with a vertically polarized input beam. Comparison of the zero power gain measured with an unpolarized and with a horizontally polarized input beam with the zero power gain measured with a vertically polarized input beam showed that polarization does not affect the zero power gain.

Zero power gain BLAZE II calculations³ showed that best agreement between the experimental and calculated zero power gains was obtained for 3.2% SF_6 dissociation and 2.5 cm secondary mixing length. Comparison of the calculated and experimental peak zero power gains showed that the calculated $P_1(J)$ peak zero power gains are about 9% smaller than the experimental ones, while the calculated $P_2(J)$ peak zero power gains are about 13% larger than the experimental ones. Comparison of the gain zones of the calculated and the experimental zero power gains showed that calculations predict gain zones that are about 30% longer than the data. The calculated $P_1(J)$ zero power gains peak 4.0 mm downstream of the H_2 injectors, while the experimental $P_1(J)$ zero power gains peak 1.5 to 2.0 mm downstream of the H_2 injectors. The calculated $P_2(J)$ zero power gains peak 2.0 mm downstream of the H_2 injectors, while the experimental ones peak 1.0 mm downstream of the H_2 injectors. The calculations predicted that the peak zero power gain lines were two J's lower than the data.

V. CONCLUDING REMARKS

A comparison of the CL I and CL II stable resonator data showed several scale effects. The CL I power was an average of 45% of the CL II power for the same cavity loss, independent of pressure. The fraction of the power in the $1 \rightarrow 0$ vibrational band did not change significantly; however, the peaks of the power spectral distributions of the CL I were shifted one J lower than the CL II spectral peaks for the same cavity loss. The CL I spectra exhibit fewer J lines than CL II spectra. These effects are a consequence of the fact that the saturated gain of the CL I laser is twice that of the CL II laser when the lasers have the same cavity loss. As observed with the CL II stable resonator data, the CL I spectra shifted toward lower J's as the pressure decreased and shifted toward higher J's as the flow rates increased.

The most interesting result was that, when the saturated gains of the two lasers were the same, the CL I power was an average of 62% of the CL II power for low pressure and 68% for high pressure. For the high SF₆ flow rates, the CL I power was 70-80% of the CL II power, independent of pressure. These data suggest that, if the saturated gain is held constant, for only a 25% performance penalty, the size, weight and gas flow rates of a laser can be reduced by a factor of 2. The power spectral distributions of the two lasers were very similar when the saturated gains of the two lasers were the same. As in the CL II data, the minimum at P₂(11) was observed in the high pressure, high SF₆ flow rate CL I data. This minimum is thought to be a consequence of a near resonant energy transfer^{6,7,9} from $v = 3, J = 3,4$ to $v = 2, J = 14$ with a subsequent rotational cascade to $v = 2, J = 11$.

Both the BLAZE II and MNORO3SR computer simulations gave good agreement with the measured CL I power, power split and beam diameters. MNORO3SR computations produced power spectral distributions which were in

reasonable agreement with the CL I data. These calculations show that the BLAZE II and MNORO3SR computer models of the Helios laser are valid as a function of mass flow rates, cavity losses, pressure and size of the laser.

The time-dependent oscillations in the output beam of the CL I Laser employing a confocal unstable resonator all had a period of about 47 ns and increased in amplitude as the fraction of the resonator filled by the saturated gain of a lasing line decreased. A 7 ns oscillation, which was superimposed on top of the 47 ns oscillation, is thought to be a mode beat of the laser. The oscillations on lines whose saturated gain does not fill the resonator did not occur for Fresnel numbers less than 3.2. Comparison of CL I and CL II unstable resonator data shows that fewer lines were observed for the CL I which is a consequence of the fact that the saturated gain of the CL I was twice as large as that of the CL II. The higher saturated gain of the CL I also is responsible for the large difference in CL I and CL II unstable resonator powers. Overall, the CL I unstable resonator data is consistent with the CL II unstable resonator data.

The most interesting result of this study was the indication that if the saturated gain is held constant, for only a 25% performance penalty, the size, weight and gas requirements of a laser can be reduced by a factor 2. This was suggested by a comparison of Helios CL I and CL II laser performance with $\alpha_{\text{sat}} = 0.0192 \text{ cm}^{-1}$. Further experiments need to be performed with other values of α_{sat} to determine if the performance penalty is a function of the magnitude of α_{sat} .

The unstable resonator modeling calculations showed that one set of baseline parameters that allow the model to predict the data as the size of the resonator and size of the laser varied could not be found. This inability to obtain one set of baseline parameters revealed limitations in the unstable

resonator model. The limitations are due primarily to the treatment of the fluid dynamic mixing. Since these limitations were not apparent in Fabry-Perot and stable resonator models with the same mixing model, the unstable resonator data as a function of resonator size and size of the laser was shown to be a severe test of a coupled, wave optics, chemical kinetic, fluid dynamic model of a chemical laser.

To improve the MNORO3UR model, the treatment of the fluid dynamic mixing should be improved. Sonic transverse injection into a subsonic multicomponent reacting shear flow results in a three-dimensional flow field. The idealization of this as a two-dimensional array of parallel, alternating fuel and oxidizer slit nozzles with subsequent linear mixing is an oversimplification. A full, three-dimensional mixing model is needed.

A mechanism that explains the time-dependent oscillations that occur on lines whose saturated gain does not fill the unstable resonator was proposed. According to the proposed mechanism, the time-dependent oscillations are the result of a competition between chemical pumping and radiative deactivation of the upper laser levels of HF. The oscillations occur only if the media is not strongly coupled to the optical fields diffractively or geometrically. Computer calculations supported the proposed mechanism. To verify the proposed mechanism, new unstable resonator experiments should be conducted. Based on the proposed mechanism, for a fixed resonator Fresnel number, the period of the time-dependent oscillations should increase as the magnification of the resonator decreases. Thus an experiment with a 4 mm slit resonator with a magnification of 1.25 (20% outcoupled) should be conducted. For this resonator, the period of the oscillations should be greater than for a 4 mm slit resonator with a magnification of 2. The proposed mechanism also predicts that the oscillation amplitude modulation

should increase and the period decrease as the Fresnel number of the resonator increases with the geometric coupling held constant. Thus experiments with mirror spacing of 200 cm and 50 cm should be performed for a 50% geometric outcoupled 4 mm slit resonator. There should be no oscillations with the 200 cm mirror spacing, except for the mode beat of the laser which should have a period of 13 to 14 nsec. With the 50 cm mirror spacing, there should be oscillations that have a larger amplitude and a shorter period than the oscillations seen with a mirror separation of 100 cm. A mode beat with the 50 cm mirror spacing should not be observed.

Preliminary amplifier experiments with 0% and 50% aperturing of the input beam by the flow channel showed that flow channel aperturing caused a significant reduction (an average of 16%) in the amplification ratio. An investigation of the multiline amplifier absorption of the input beam showed that He and O₂ did not absorb and that the SF₆ absorption was less than 0.005 cm⁻¹. Thus, all amplifier experiments were performed with no flow channel aperturing of the input beam and the effect of SF₆ absorption could be neglected.

Multiline amplification experiments showed that the peak amplification ratios occurred at an X₀ that is both close to the values of X₀ for peak power when a stable resonator is used on the CL II, and close to the values of X₀ at which the peak zero power gains of the P₁(J) and P₂(J) lines were measured. Thus, to obtain maximum amplification, the input beam should be passed through the amplifier at the X₀ location corresponding to peak amplifier gain. Higher amplification ratios were obtained when both the oscillator and the amplifier were run at the Run 34 flow rates than when both were run at the Run 36 flow rates. This was a consequence of the higher input intensity that was used in the case of the Run 36 flow rates.

Preliminary single-line amplification experiments showed that the peak $P_1(6)$ and $P_2(6)$ amplification ratios occurred at the same X_c at which the zero power gains are a maximum. Thus, to obtain maximum single-line amplification, the input beam should be passed through the amplifier at the X_c for maximum zero power gain. The single-line amplification ratios were considerably lower than the multi-line amplification ratios that were measured using the same input power. This was a result of the fact that in the multiline case, the total input power was distributed among the different lasing lines, which means that the input intensity on each line was less than the input intensity in the single-line case. This fact resulted in higher amplification ratios for each line, because each line's gain in the amplifier was depressed less than in the single-line case for the same total input power.

The multiline amplifier performance was measured as a function of input power. It was found that about 1/3 of the oscillator output needs to be input to obtain amplifier output equal to the oscillator performance.

The amplifier input power required to measure the zero power gain of each line was obtained by measuring the amplification ratio as a function of input power at the point in the flow field corresponding to maximum amplification. When the amplification ratio became independent of input power, the zero power gain region had been reached. The zero power gain of each line was then measured for the low pressure Run 34 and Run 36 flow rates as a function of x and it was found that the $P_2(J)$ peak zero power gains are about 1.55 times larger than the $P_1(J)$ peak zero power gains. The length of the gain zone of the $P_1(J)$ lines is about 1.3 times larger than that of the $P_2(J)$ lines.

The zero power gains of all the $P_1(J)$ lines reached their peak 1.5 - 2.0 mm downstream of the H_2 injectors while the zero power gains of the $P_2(J)$

lines reached their peak 1.0 mm downstream of the H₂ injectors. The lines with the highest zero power gains are P₁(5) and P₁(6) for the 1 → 0 vibrational band and P₂(5) and P₂(6) for the 2 → 1 vibrational band. The variation of zero power gain with height in the flowfield was investigated by taking P₂(5) zero power gain measurements with the Run 34 flow rates in the amplifier at the center line of the flow channel, and ± 0.75 mm above and below the center line of the flow channel. The zero power gain values obtained 0.75 mm above and below the center line of the flow channel were almost identical and higher than the zero power gain values measured on the flow channel centerline. This was due to the way the primary and the secondary streams mix after injecting H₂ from the upper and lower flow channel walls.

The effects of high pressure on zero power gain were investigated for lines P₁(6), P₂(5) and P₂(6); it was found that high pressure results in gain zones that are considerably shorter than those measured in the case of low pressure. The peak zero power gain of P₁(6) was not affected by high pressure but the peak zero power gains of P₂(5) and P₂(6) were decreased by almost 22.5%. High pressure caused the location of the peak zero power gain to occur 0.5 mm closer to the H₂ injectors for all three lines.

The effect of polarization on zero power gain was studied by comparing zero power gain data taken with vertically polarized, horizontally polarized, and unpolarized beams. It was found that polarization does not affect zero power gain.

The best agreement between the experimental and the calculated³ zero power gains was obtained when a 3.2% SF₆ dissociation and a secondary mixing length of 2.5 cm were used. Comparison of the experimental and the calculated peak zero power gains showed that the calculated P₁(J) peak zero power gains

are about 9% smaller than the experimental ones. The calculated $P_2(J)$ peak zero power gains are about 13% larger than the experimental ones. Calculations predicted gain zones that are about 30% longer than those measured experimentally. The calculated $P_1(J)$ zero power gains peak 4.0 mm downstream of the H_2 injectors, while the experimental $P_1(J)$ zero power gains peak 1.5 to 2.0 mm downstream of the H_2 injectors. The calculated $P_2(J)$ zero power gains peak 2.0 mm downstream of the H_2 injectors, while the experimental ones peak 1.0 mm downstream of the H_2 injectors. Calculations predicted that the peak zero power gain lines are two J's lower than the data. The difference between the calculated and measured zero power gains are a consequence of approximating the three dimensional flow field with a one dimensional scheduled mixing model.

REFERENCES

1. L. H. Sentman, P. Theodoropoulos and A. Gumus, "Mass Flow Calibration of the Helios CL I and CL II Laser Control Consoles," AAE TR 86-4, UILU ENG 86-0504, Aeronautical and Astronautical Engineering Department, University of Illinois, Urbana, IL, August 1986.
2. L. H. Sentman, D. L. Carroll, P. Theodoropoulos and A. Gumus, "Scale Effects in a cw HF Chemical Laser," AAE TR 86-5, UILU ENG 86-0505, Aeronautical and Astronautical Engineering Department, University of Illinois, Urbana, IL, September 1986.
3. L. H. Sentman and J. O. Gilmore, "Computer Simulation of cw HF Chemical Laser Unstable Resonator Performance," AAE TR 87-5, UILU ENG 87-0505, Aeronautical and Astronautical Engineering Department, University of Illinois, Urbana, IL, August 1985.
4. L. H. Sentman, P. Theodoropoulos, R. Waldo, T. Nguyen and R. Snipes, "An Experimental Study of cw HF Chemical Laser Amplifier Performance and Zero Power Gain," AAE TR 87-6, UILU ENG 87-0506, Aeronautical and Astronautical Engineering Department, University of Illinois, Urbana, IL, August 1987.
5. L. H. Sentman, D. Carroll, J. Gilmore, P. Theodoropoulos, R. Waldo and A. Gumus, "CW HF Chemical Laser MOPA Performance," AIAA preprint 87-1449, 19th Fluid Dynamics, Plasma Dynamics and Lasers Conference, June 8-10, 1987, Honolulu, Hawaii.
6. L. H. Sentman, P. Renzoni and S. Townsend, "The Effects of Cavity Losses on the Performance of a Subsonic cw HF Chemical Laser," AAE TR 83-7, UILU ENG 83-0507, Aeronautical and Astronautical Engineering Department, University of Illinois, Urbana, IL, June 1983.

7. L. H. Sentman, M. H. Nayfeh, P. Renzoni, K. King, S. Townsend and G. Tsioulos, "Saturation Effects in a cw HF Chemical Laser," AIAA Journal, Vol. 23, No. 9, 1985, pp. 1392-1401.
8. L. H. Sentman, M. H. Nayfeh, S. W. Townsend, K. King, G. Tsioulos and J. Bichanich, "Time-Dependent Oscillations in a cw Chemical Laser Unstable Resonator," Applied Optics, Vol. 24, No. 21, November 1, 1985, pp. 3598-3609.
9. L. H. Sentman, G. Tsioulos, J. Bichanich and D. Carroll, "An Experimental Study of Fabry-Perot and Stable Resonator cw HF Chemical Laser Performance," AAE TR 85-3, UILU ENG 85-0503, Aeronautical and Astronautical Engineering Department, University of Illinois, Urbana, IL, March 1985.
10. L. H. Sentman, W. O. Mosebach and P. Renzoni, "A Theoretical and Experimental Study of cw HF Chemical Laser Performance," AAE TR 81-8, UILU ENG 81-0508, Aeronautical and Astronautical Engineering Department, University of Illinois, Urbana, IL, December 1981.
11. L. H. Sentman and P. Schmidt, "MNOR03; An Efficient Rotational Nonequilibrium cw HF Chemical Laser Model," AAE TR 83-1, UILU ENG 83-0501, Aeronautical and Astronautical Engineering Department, University of Illinois, Urbana, IL, January 1983.
12. L. H. Sentman, P. F. Schmidt and G. M. Marinos, "Effects of the HF Rate Package and the Optical Resonator on cw HF Chemical Laser Performance," AAE TR 83-6, UILU ENG 83-0506, Aeronautical and Astronautical Engineering Department, University of Illinois, Urbana, IL, June 1983.
13. L. H. Sentman, J. D. Bichanich, D. Carroll, V. Coverstone and P. Theodoropoulos, "Simulation of Fabry-Perot and Stable Resonator cw HF

- Chemical Laser Performance," AAE TR 85-6, Aeronautical and Astronautical Engineering Department, University of Illinois, Urbana, IL, September 1985.
14. J. W. Raymond, M. Subbiah, J. T. Schimke, S. W. Zelazny and L. H. Sentman, "Advanced HF and DF Chemical Laser Performance Modeling, Vol. I, The CNCDE/BLAZE Rotational Equilibrium Code," TR DRCPM-HEL-CR-79-7, Bell Aerospace Textron, Buffalo, NY, 1979.
 15. L. H. Sentman, M. Subbiah and S. W. Zelazny, "BLAZE II, A Chemical Laser Simulation Program," TR H-CR-77-8, Bell Aerospace Textron, Buffalo, NY, 1977.
 16. L. H. Sentman, G. Tsioulos, J. Bichanich, D. Carroll, P. Theodoropoulos, J. Gilmore and A. Gumus, "A Comparative Study of cw HF Chemical Laser Fabry-Perot and Stable Resonator Performance," Proceedings, International Conference on Lasers, '85, Las Vegas, Nevada, 2-6 December 1985 (STS Press, McLean, VA, 1986).
 17. L. H. Sentman, M. H. Nayfeh, W. O. Mosebach, P. Renzoni, K. Herrick, K. King, P. Schmidt and S. Townsend, "Theoretical and Experimental Study of cw HF Chemical Laser Performance," Proceedings, Fourth International Symposium on Gas Flow and Chemical Lasers, Stresa, Italy, 13-17 September 1982 (Plenum, NY, 1985).
 18. L. H. Sentman, S. Townsend, G. Tsioulos, J. Bichanich, M. Nayfeh and K. King, "Time-Dependent Oscillations in a cw HF Chemical Laser Unstable Resonator, AAE TR 84-2, UILU ENG 84-0502, Aeronautical and Astronautical Engineering Department, University of Illinois, Urbana, IL, May 1984.
 19. R. Gross and J. Bott, Handbook of Chemical Lasers, Ch. 2, pp. 118-119, John Wiley, New York, 1976.

20. L. H. Sentman and M. H. Nayfeh, "Nonlinear Interaction Between the Pumping Kinetics, Fluid Dynamics and Optical Resonator of cw Fluid Flow Lasers," AAE TR 83-5, UIIU ENG 83-0505, Aeronautical and Astronautical Engineering Department, University of Illinois, Urbana, IL, March 1983.